



A Model of Hydrothermal Dolomite Reservoir Facies in Precambrian Dolomite, Central Sichuan Basin, SW China and its Geochemical Characteristics

GU Yifan¹, ZHOU Lu¹, JIANG Yuqiang^{1,*}, JIANG Chan², LUO Mingsheng³ and ZHU Xun⁴

¹ School of Geosciences & Technology, Southwest Petroleum University, Chengdu 610500, China

² Exploration Division, PetroChina Southwest Oil & Gas Field Company, Chengdu 610041, China

³ Shunan Division of PetroChina Southwest Oil & Gas Field Company, Luzhou 646000, Sichuan, China

⁴ Exploration and Development Institute of Southwest Oil & Gas Field Company, PetroChina, Chengdu 610041, China

Abstract: Hydrothermal mineral assemblages and related hydrothermally enhanced fracturing are common in the Precambrian Dengying Formation of Central Sichuan Basin. Petrographic and geochemical analyses of core samples show that the hydrothermal dolomite reservoirs of Dengying Formation consist of four main types of pores in the reservoir facies. These include: 1) hydrothermal dissolution vug (or pore), 2) intercrystalline pore, 3) residual inter-breccia vug (or pore), and 4) enlarged dissolved-fracture. There are three different fabrics dolomite in hydrothermal dolomite reservoirs, namely, saddle dolomite, fine-medium dolomite and micritic dolomite. Micritic dolomite is the original lithology of host rock. Saddle dolomite with curved or irregular crystal faces was directly crystallized from hydrothermal fluids (average temperature 192°C). Fine-medium dolomites are the products of recrystallization of micritic dolomite, resulting in abnormal geochemical characteristics, such as slight depletion of $\delta^{18}\text{O}$, significant enrichment of Mn-Fe and $^{87}\text{Sr}/^{86}\text{Sr}$, and positive Eu anomaly. A model for the distribution of various hydrothermal dolomite reservoir facies is proposed here, which incorporates three fundamental geological controls: 1) extensional tectonics and tectono-hydrothermal events (i.e., the Xingkai Taphrogenesis of Late Sinian-Early Cambrian, and Emei Taphrogenesis of Late Permian), 2) hydrothermal fluid storage in clastic rocks with large thickness (e.g., Nanhua System of Chengjiang Formation and part of Doushantuo Formation), and 3) confining bed for hydrothermal fluids (such as, the shale in Qiongzhusi Formation). The supply of hydrothermal fluid is critical. Large basement-rooted faults and associated grid-like fracture system may function as the channels for upward migration of hydrothermal fluid flow. The intersection of the above-mentioned faults (including the conversion fault), especially transtensional sags above negative flower structures on wrench faults can serve as a key target for future hydrocarbon exploration.

Key words: hydrothermal dolomite, reservoir facies, geochemical characteristics, Precambrian, Dengying Formation, central Sichuan Basin

Citation: Gu et al., 2019. A Model of Hydrothermal Dolomite Reservoir Facies in Precambrian Dolomite, Central Sichuan Basin, SW China and its Geochemical Characteristics. *Acta Geologica Sinica* (English Edition), 93(1): 130–145. DOI: 10.1111/1755-6724.13641

1 Introduction

The concept of hydrothermal dolomite (HTD) reservoir facies was first proposed by Davies and Smith Jr. (2006) and was later further characterized by Davies et al. (2006). These reservoir rocks are the diagenetic products of original limestone altered by hydrothermal fluids (temperature higher than the host formation at least 5°C and very saline) through a series of diagenesis such as, dissolution, replacement and recrystallization (Davies et al., 2006). The first large oil and gas reserve/production in HTD was reported from Albion-Scipio field of the northeastern United States (Hurley and Budros, 1990). Over the last 25 years, there has been an escalating focus on structurally controlled hydrothermal dolomite (HTD) reservoirs globally (Davies et al., 2006). The hydrothermal fluids replacement of limestone strata has been reported

from Miocene strata in the Tepusquet region and Ordovician strata in Wisconsin arch of United States (Malone et al., 1996; Luczaj et al., 2006), Pliocene strata in the Izu Peninsula of Japan (Matsumoto et al., 1988), Silurian strata in the Quebec region of Canada (Lavoie et al., 2004), Jurassic strata of Southern Alps region in Italy (Cervato et al., 1990; Ronchi et al., 2012), Lower Palaeozoic strata of Northern Spain and Cretaceous strata of Iraq (Shah et al., 2012; Lapponi et al., 2013; Zhang Tao et al., 2015). The HTD reservoirs now has become the important targets for oil and natural gas exploration in limestone stratum of North America (Lonnee and Machel, 2007), Canada (Qing et al., 1992; Conliffe et al., 2009; Lavoie et al., 2010), and West Asia (Nurkhanuly et al., 2014). Liu Shugen et al. (2007) considered that the host dolomite of Dengying Formation had undergone destructive diagenesis such as early compaction, sparkling cementation in the window-like holes and early-stage

* Corresponding author. E-mail: xnsyjyq3055@126.com

silicification. All the above studies suggest that the Dengying Formation, as an ancient-deep sedimentary strata, has undergone multi-stage fluid transformation including hydrothermal fluids. However, the diagenetic sequence and corresponding reservoir spaces involved with the transformation of compact host rock by hydrothermal fluids have not been systematically studied; Wang Guozhi et al. (2014) held that apart from the meteoric fresh water in the epigenetic environment, multi-stage acidic fluids play an important role in the formation of pores during the diagenesis process; According to the petrological and geochemical characteristics, Jiang Yuqiang et al. (2016) and Feng Mingyou et al. (2016; 2017) proved that there were hydrothermal fluids in the Dengying Formation in Central Sichuan, and the influence of hydrothermal fluid on the porosity of host rock was preliminarily discussed.

The Upper Sinian (Ediacaran) Dengying Formation is considered as a significant discovery of natural gas exploration in deep marine carbonate stratum (Xu Fanghao et al., 2016). In recent years, researchers generally reported that the formation of Dengying Formation dolomite reservoirs consisted of two major steps. Firstly, the growth of the microbial mounds had to overcome the strong hydrodynamic force at the platform-margin. Secondly, tectonic uplift of Tong Wan until Late Sinian (Ediacaran) followed by supergene karstification resulted in significant reworking of the microbial mounds. Therefore, vertically, the distribution of the Dengying karst reservoirs is concentrated in the upper part to the top of Dengying Formation, and its lateral distribution is mainly controlled by the distribution of the microbial mounds (or grains) and the karst geomorphic units (Li Qigui et al., 2013; Yang Wei et al., 2014; Wang Guozhi et al., 2014; Luo Bing et al., 2015). However, according to the drilling test data and results of the core studies, some of the cored wells intersected good quality reservoirs even beyond the above mentioned geological settings. These wells were drilled neither in the areas where paleo-environments were favorable for development of microbial mounds (or grains) (Lin Xiaoxian et al., 2017), nor any typical karst signature was observed in the cores. However, the reservoir sections in these wells exhibit large thickness, good porosity and high permeability. This shows that understanding of development of good quality HTD needs to be further improved for exploration of oil and gas in such reservoirs. Therefore, this study mainly focuses on the geological development and geochemical characteristics of high quality HTD reservoirs of non-karst origin in Dengying Formation. The results and conclusions from this study will help to better define the formation mechanism of deep marine reservoir in Sichuan Basin.

2 Geologic Setting

Due to multi-stage Tongwan movement, the Dengying Formation in study has experienced two significant meteoric karst events. The Dengying Formation in the study area is characterized by three fundamental geological conditions favorable for the occurrence of

hydrothermal activity.

The Xingkai Taphrogenesis of Late Sinian-Early Cambrian and Emei Taphrogenesis of Late Permian: Both were characterized by extensional movements and significant tectono-hydrothermal events, forming typical inter layered volcanics and clastic sedimentary deposits of Sinian and Permian age (Liu Shugen et al., 2008). These extensional tectonic movements were favourable for the basement-rooted faulting activity which leads to the conduits for upward migration of hydrothermal fluids.

Porous clastic rock stratum underlying the Dengying Formation: Latest three-dimensional seismic data shows that there still exist thick sedimentary strata underlying the Sinian Dengying Formation in the study area, which are mainly composed of the sandy-pebbly clastic rocks of Nanhua System Chengjiang Formation and part of Doushantuo Formation, with a thickness about 3000–5000m (Zhang Jian et al., 2012). These clastic rock strata could act as the hydrothermal fluid storage for the tectonic-hydrothermal activity of the Dengying Formation dolomite. Under extensional tectonic setting, when deep-faulting began, the hydrothermal fluids would migrate upward from the storage along faults and concomitant fractures.

Sealing shale on top of the Dengying Formation: The Lower Cambrian Qiongzhusi Formation that has unconformable contact with the underlying Sinian Dengying Formation is composed of black carbonaceous shale with 200–300 m thickness (Jiang Yuqiang et al., 2016). Consequently, the Qiongzhusi Formation is an ideal confining bed for hydrothermal fluids, constraining the hydrothermal fluids in the Dengying Formation dolomite for a significant amount of time to allow for hydrothermal reactions, rather than migrating upward or dissipating.

3 Location, Stratigraphy and Methodology

The study area is located in the Central Sichuan Basin, in which the Dengying Formation conformably overlies shales of Sinian (Ediacaran) Doushantuo Formation and is unconformably overlain by Lower Cambrian Qiongzhusi Formation shale (Liu Yifeng et al., 2014). Regional transgressive cycles and tectonic events have subdivided the Dengying Formation into four members, i.e., the 1st, 2nd, 3rd and 4th members from bottom to top, respectively (Wang Guozhi et al., 2014). 3rd member is composed of argillutite intercalated with quartz sandstone (Zi Jinping et al., 2017), while the 1st, 2nd and 4th members are all composed of microbial dolomite, micritic dolomite and crystalline dolomite, etc. (Fig. 1). The 4th member deposits can be divided into two facies: platform-margin facies, which is mainly composed of microbial mounds or grains, and interior-platform facies, which is primarily composed of micritic dolomites (Fig. 2).

Cores from 30 cored-wells were analyzed with a goal to document the petrological characteristics of dolomite. Over 100 core samples of dolomite reservoirs were doubly polished, followed by blue epoxy-impregnation and staining with Alizarin red for microscopic identification. Twenty three thin-sections were prepared for fluid-

inclusion work. The remaining samples were utilized to select fresh sections, avoid calcite veins and organic matter, and grind them to 200 meshes for rare earth elements (REE), trace elements, strontium isotopes, carbon and oxygen isotopes analyses. The REE (14 samples) were analyzed using inductively-coupled plasma mass spectrometer, of which the limit of detection (unit: $\mu\text{g/g}$) are: Ce: 0.05–500, Dy: 0.02–50, Er: 0.01–50, Eu: 0.01–50; Gd: 0.05–50, Ho: 0.01–50, La: 0.05–500, Lu: 0.02–50, Nd: 0.05–100, Pr: 0.01–100, Sm: 0.02–50, Tb: 0.03–50, Tm: 0.03–50, Yb: 0.01–50. Considering the relationship between carbonate diagenetic fluids and normal seawater, this study selects REE content of seawater published by Kawabe et al. (1998) as standard. Because REE contents of seawater are very low, the REE contents of seawater are magnified by 104 times before standardization. Trace elements (20 samples) were analyzed using atomic absorption spectrometer (test

conditions: temperature 20°C, humidity 60%) with standard deviation 0.0004–0.0032 mg/L and detection limit is 0.0003 mg/L and all trace elements datum were converted to 10^{-6} . Eleven stable isotopic ($\delta^{18}\text{O}$, $\delta^{13}\text{C}$) and five $^{87}\text{Sr}/^{86}\text{Sr}$ analyses of different fabrics dolomite were carried out at SWPU using the carbonate reaction method. Samples were reacted by the application of the phosphoric acid bath method at 90°C, and then CO_2 generated was examined through use of Elementar IsoPrime GC5. Standard isobaric corrections were adopted, while strontium was separated using the Eichrom SR-specres and measured on a Triton plus thermal ionization mass spectrometer. All stable isotope data are converted to Vienna Pee Dee Belemnite (V-PDB) and corrected by fractionation factors supplied by Fairchild and Spiro (1987). Precision of the $\delta^{18}\text{O}$ and $\delta^{13}\text{C}$ ratios data is better than $\pm 0.1\%$. The fluid-inclusion measurement of Goldstein and Reynolds (1994) was employed for

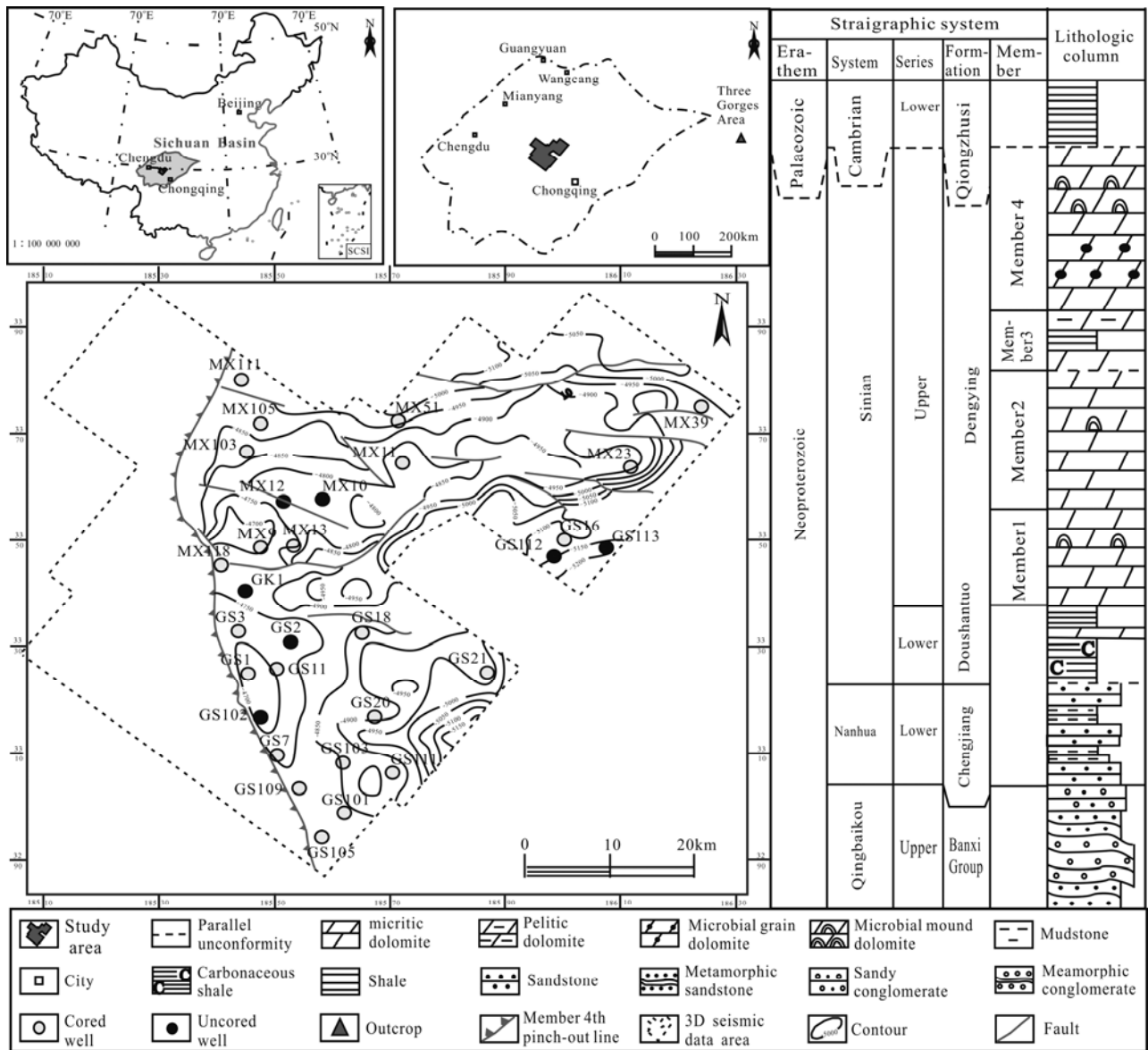


Fig. 1. Location map and stratigraphic column of the study area, central Sichuan Basin (China basemap after China National Bureau of Surveying and Mapping Geographical Information).

experimentation, which involved the use of a Linkam THMSG600 system (testing range: $-196-600^{\circ}\text{C}$, accuracy: 0.2°C). Cathodoluminescence was detected with CL8200MK5 type cathodoluminescence microscope.

4 Evidence of Hydrothermal Activity

4.1 Petrographic evidence

4.1.1 Hydrothermal mineral assemblages

Hydrothermal activity caused by basement faulting is often associated with the formation of Mississippi Valley type (MVT) hydrothermal mineral assemblages (Luczaj, 2006; Ostendorf et al., 2016; Jiang Yuqiang et al., 2016). The most common hydrothermal minerals are saddle dolomite (SD), galena (Gn), sphalerite (Sp), pyrite (Py), barite (Brt), fluorite (Fl), feldspar (Fsp) and quartz (Qtz). However, these minerals could also be of non-hydrothermal origin. Therefore, instead of occurrence of individual minerals, an assemblage of minerals should be utilized to establish whether a region has hydrothermal activity history. For example, the hydrothermal mineral assemblages that characterize: 1) the Tarim Basin of China are quartz-fluorite and sphalerite-calcite-chlorite (Jin Zhijun et al., 2006; Pan Liyin et al., 2009; Zhu Dongya et al., 2010; Liu Wei et al., 2016); 2) the Red Sea area of Egypt are montmorillonite-sphalerite-hematite-gypsum, and goethite-sphalerite-pyrite-anhydrite (Cocherie et al., 1994), the south-central New York of U.S. are quartz-saddle dolomite-authigenic feldspar (Smith Jr., 2006) and the Zagros Basin of Iraq are saddle dolomite-celestine-anhydrite etc (Zhang Tao et al., 2015). This study reveals that the hydrothermal mineral assemblages characteristic of the Dengying Formation in the study area are saddle dolomite-galena-sphalerite (Fig. 3a), saddle dolomite-quartz-sphalerite (Fig. 3b), galena (Fig. 3c)-sphalerite-pyrite (Figs. 3d and 3e), saddle dolomite-pyrite-quartz (Fig. 3f) and saddle dolomite-quartz-anhydrite (Fig. 3g). These mineral occurs mainly as fillings in vugs or fractures as observed on the cores (Fig. 3). Differences in types of hydrothermal mineral assemblages may indicate differences in sources and types of hydrothermal fluids.

Zebra-like fabric is common near shear faults, especially in the footwall of extensional faulting environment (Tarasewicz et al., 2005). It is always associated with hydrothermal activity (Lapponi et al., 2013), recording the transient shear stress and the release of pore fluid pressure. When a rock stratum suddenly breaks due to abrupt faulting, the pressure surrounding the break point drops sharply, but the pore fluid pressure in compact micritic dolomite with low permeability cannot be released immediately. Thus, “explosive fracturing”, also known as “hydraulic fracturing” will take place in the position where the pore fluid pressure is much higher than the surrounding pressure (Phillips, 1972; Roehl, 1981). With the happening of hydraulic fracturing, there is a dramatic drop of hydrothermal fluid pressure that the saddle dolomite precipitated out of hydrothermal fluids will rapidly fill the micro-fractures, pores and vugs created by the “explosive fracturing” and consequently form the zebra-like fabric (Fig. 4a). The origin of the dilational breccia fabric is extremely similar to zebra-like fabric but

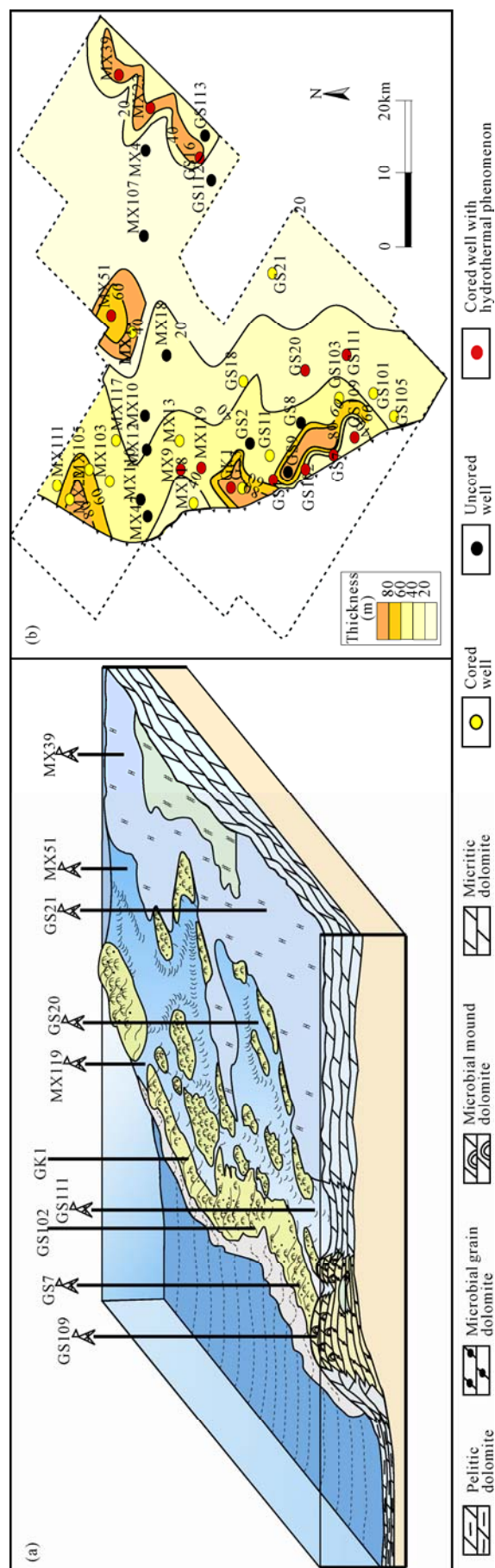


Fig. 2. Sedimentary paleo-environment map (a) and thickness distribution map of high quality reservoir (net reservoir thickness with porosity $>3\%$) (b) of the Dengying Formation member 4th in the study area.

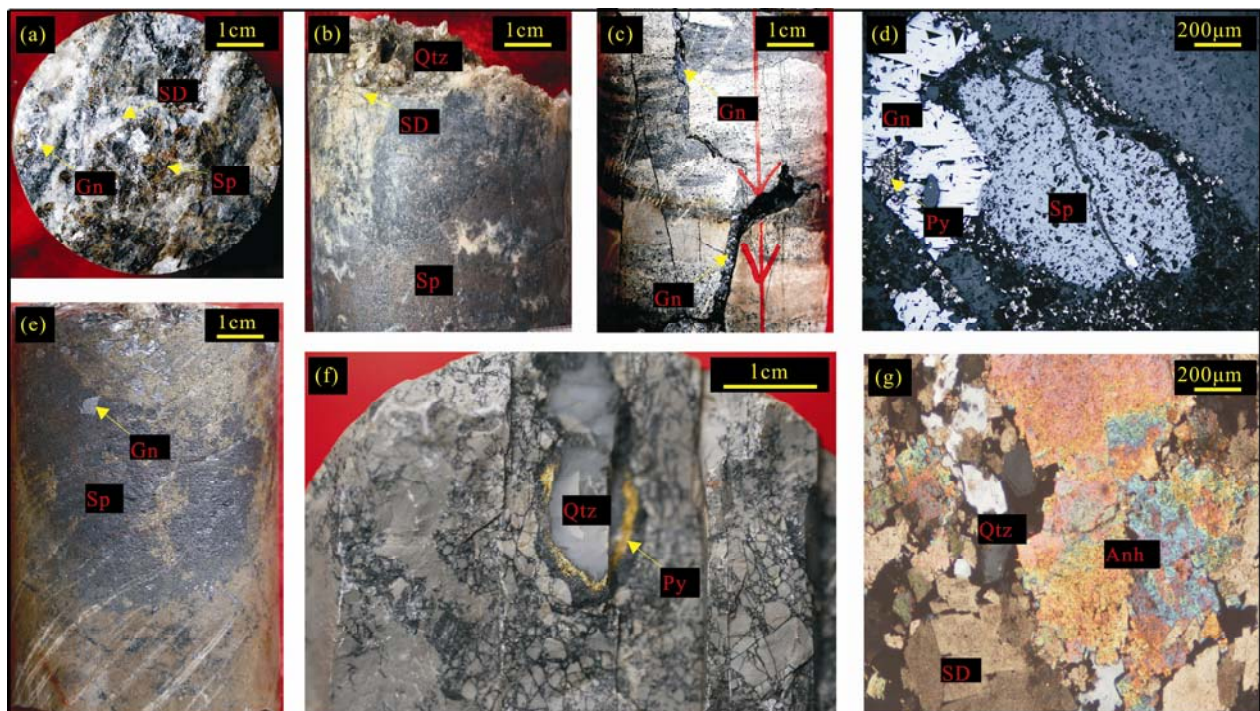


Fig. 3. Petrographic characteristics of hydrothermal mineral assemblage.

(a) Saddle dolomite (SD)-galena (Gn)-sphalerite (Sp), Well GS109, 5316.06 m; (b) quartz (Qtz)-saddle dolomite (SD)-sphalerite (Sp), Well GS102, 5043.97 m; (c) galena (Gn) filled in near vertical fracture, Well MX51, 5385 m; (d) hydrothermal mineral assemblages of galena (Gn)-sphalerite (Sp)-pyrite (Py) in dissolved pore, Well MX9, 5444.5 m, reflected light; (e) galena (Gn)-sphalerite (Sp) filled in dissolved vug, Well GS101, 5517.2 m; (f) quartz (Qtz)-pyrite (Py) filled in dissolved vug, Well MX39, 5309.3 m; (g) quartz (Qtz)-anhydrite (Anh)-saddle dolomite (SD), Well GS1, 4956.3 m, cross-polarized light.

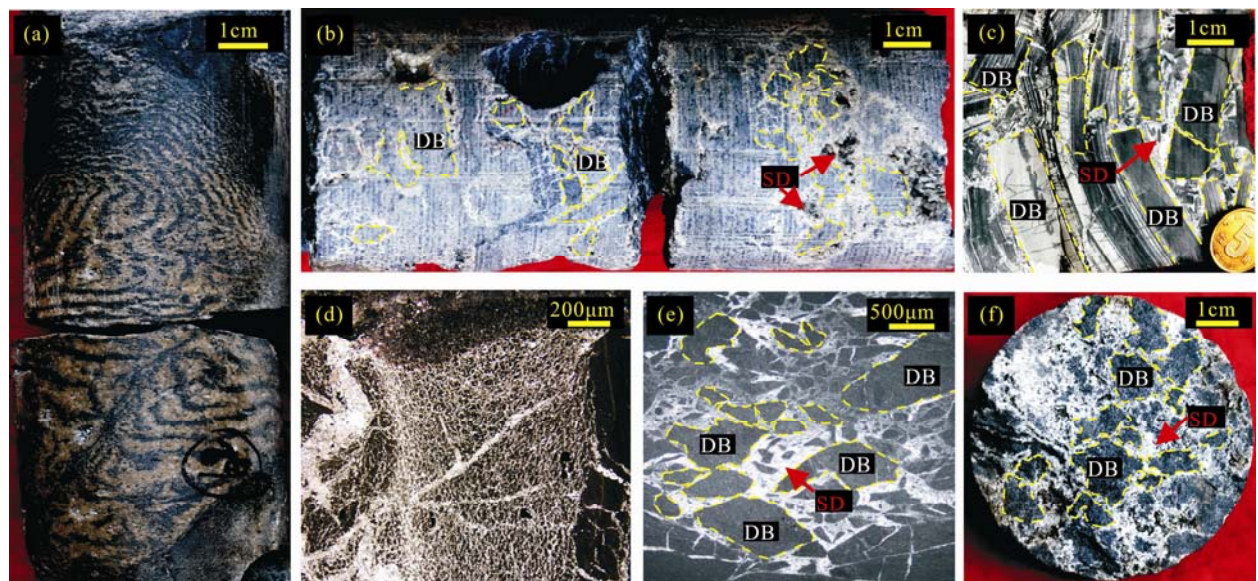


Fig. 4. Petrographic characteristics of zebra-like fabric and dilational breccia fabric.

(a) Zebra-like fabric, Well GS111, 5324.02–5302.17 m; (b) dilational breccias (DB) fabric, Well MX51, 5334.4 m; (c) dilational breccias (DB) fabric, Well GS20, 5182.48 m; (d) zebra-like fabric, Well GS20, 5185.38–5185.58 m, plane-polarized light; (e) dilational breccias (DB) fabric, Well MX39, 5309.2 m, plane-polarized light; (f) dilational breccias (DB) fabric, Well GS1, 4972.7 m.

the former fabric is apparently much larger than the latter (Figs. 4b and 4c). Unlike the karst breccias, the composition of the dilational breccias is homogeneous and all of these breccias are compact micritic dolomite (host rock) (Figs. 4d and 4e). Moreover, there is no overlying sediments or vadose silts between these breccias. All

dilational breccias float in the saddle dolomite cements with an angular shape and usually exhibit a collage (Fig. 4f).

4.2 Geochemical evidence

4.2.1 Fluid-inclusions

Twenty-three two-phase (gas-liquid) primary fluid-

inclusions from saddle dolomite (D3), fine-medium dolomite (D2) and quartz cement (Q1) were analyzed. The test results indicate that the homogenization temperature (T_h) of D3 ($n=18$) ranges from 140 to 230°C (average value=192°C); the homogenization temperature in D2 ($n=32$) ranges from 101 to 152°C (average value=125°C) (Feng et al., 2017); the T_h distribution of Q1 ($n=5$) ranges from 196 to 230°C (average value=215°C) (Fig. 5).

According to the simulation curve of burial and thermal history of Well GK1 in the study area (Fig. 6), it is illustrated that the normal formation temperature of Dengying Formation member 4th is 50–70°C and 100–160°C respectively when underwent two major tectonic-hydrothermal events (Xingkai Taphrogenesis and Emei Taphrogenesis). Obviously, the homogenization temperatures of D3 and Q1 are much higher than D2 and the normal formation temperature of Dengying Formation (Fig. 5). And laser-Raman testing of saddle dolomite of Dengying Formation in South eastern Sichuan Basin illustrate that the gas phase of gas-liquid fluid-inclusions in saddle dolomite consist of CO₂, CH₄, H₂S and N₂, and corresponding liquid phase consist of H₂O and CO₂. In addition, CO₂ in the liquid phase accounted for 13.6%–28.3%, in the gas phase accounted for 26.9% to 67.4% (Song Guangyong et al., 2011). All the test results demonstrate that the hydrothermal fluids in the study area are CO₂-enriched, acidic fluids and with high temperature. Thus, this kind of fluids is able to strongly dissolve compact micritic dolomite such as of Dengying Formation (the host rock).

4.2.2 Strontium, oxygen and carbon isotopes

Previous research shows that the distribution of ⁸⁷Sr/⁸⁶Sr

value ranges from 0.7085 to 0.7087 (average value=0.7086, $n=3$) in marine limestone of Dengying Formation and in micritic dolomite those values range from 0.709123 to 0.709971, respectively (average value=0.7096, $n=5$) (Yang et al., 1999). By comparison, the test results of this paper illustrate that the ⁸⁷Sr/⁸⁶Sr value of micritic dolomite ranges from 0.7089 to 0.7097 (average value=0.7092, $n=5$) that is similar to previous research; the ⁸⁷Sr/⁸⁶Sr value of fine-medium dolomite ranges from 0.7103 to 0.7106 (average value=0.7105, $n=4$); the ⁸⁷Sr/⁸⁶Sr value in saddle dolomite ranges from 0.7114 to 0.7132 (average value=0.7119, $n=7$). Therefore, fine-medium dolomite and especially the saddle dolomite have higher ⁸⁷Sr/⁸⁶Sr value, compared to marine limestone and micritic dolomite (Table 1). This phenomenon is caused by the reaction of hydrothermal fluids with clastic sediments and basement rocks containing mud and / or feldspar. The greater the water-rock reaction between hydrothermal fluids and carbonate is, the higher the enrichment of radioactive ⁸⁷Sr is (Qing et al., 1992; 1994).

The distribution characteristics of $\delta^{18}\text{O}$ value is very similar to that of ⁸⁷Sr/⁸⁶Sr value that the $\delta^{18}\text{O}$ values from high to low are Sinian (Precambrian) paleo-seawater (–0.50‰) (Huang Zhicheng et al., 1999), micritic dolomite (average value=–2.87‰, $n=5$), fine-medium dolomite (average value=–9.13‰, $n=9$) and saddle dolomite (average value=–11.00‰, $n=7$) (Fig. 7b). This phenomenon can be attributed to the thermal fractionation effect on the process of the diagenesis involving hydrothermal fluids. The higher the temperature of diagenetic reaction or crystallization process, the further the reduction of the $\delta^{18}\text{O}$, which is explained as the result of recrystallization of micritic dolomite under the

Table 1 Trace-element composition, C, O stable isotopes and Sr isotopic ratio of different dolomite fabrics for Dengying Fm.

Sample identification					Stable isotopes		Trace elements		Rad. Isotopes
Sample No.	Well No.	Fm.	Depth (m)	Fabric type	$\delta^{13}\text{C}$ (‰)	$\delta^{18}\text{O}$ (‰)	Fe (ppm)	Mn (ppm)	⁸⁷ Sr/ ⁸⁶ Sr
1	GS1	Member 4th	4 984.7	D1	0.86*	–4.28*	152	88	
2	GS1	Member 4th	4 985	D1	1.93*	–3.63*	72	109	0.7097*
3	GS1	Member 4th	4 972.7	D1			70	841	
4	MX9	Member 4th	5 042.6	D1			59	171	
5	MX9	Member 4th	5 433.5	D1			18	80	0.7089
6	MX39	Member 4th	5 303.5	D1	–0.46	–5.37	18	160	0.7089
7	MX39	Member 4th	5 303.7	D1	1.99	0.89	43	314	0.7094
8	MX39	Member 4th	5 302.9	D1	0.19	–1.95	135	160	0.7097
9	GS16	Member 4th	5 450.3	D2	–1.93	–13.84	371	930	
10	GS16	Member 4th	5 450.6	D2	–0.43	–13.69	—	601	
11	GS1	Member 4th	4 972.1	D2			232	670	
12	GS1	Member 4th	4 974.6	D2			216	363	
13	GS1	Member 4th	4970.4	D2	1.34*	–7.98*	821*	654*	0.7103*
14	MX9	Member 2nd	5318.2	D2	0.13*	–5.38*	501*	134*	0.7106*
15	MX9	Member 4th	5431.2	D2	0.45*	–9.63*	139*	196*	0.7105*
16	MX119	Member 4th	4967.1	D2	–0.17*	–7.19*	320*	640*	0.7106*
17	MX39	Member 4th	5 286.2	D2	0.48	–6.56	385	156	
18	MX51	Member 4th	5 332.6	D2	0.84	–12	1946	1707	
19	MX51	Member 4th	5 391.2	D2	0.84	–5.92	373	301	
20	GS7	Member 4th	5 346.1	D3	–0.31	–14.6	911	579	
21	GS7	Member 4th	5 346	D3	0.51	–12.24	750	852	0.7114*
22	GS6	Member 4th	5 383.7	D3			1882	736	
23	MX9	Member 4th	5 440.2	D3			351	758	0.7117*
24	GS1	Member 4th	4956.3	D3	0.59*	–9.85*			0.7114*
25	GS1	Member 4th	4656.3	D3	–0.52*	–9.75*			0.7128*
26	GS1	Member 4th	4967.5	D3	2.94*	–6.8*	1932*	855*	0.711*
27	GS1	Member 4th	4971	D3	0.67*	–12.34*	2457*	976*	0.7122*
28	GS1	Member 4th	4974.1	D3	–2.16	–11.43	2438	823	0.7132

Note: *data cited from Feng Mingyou et al., 2017.

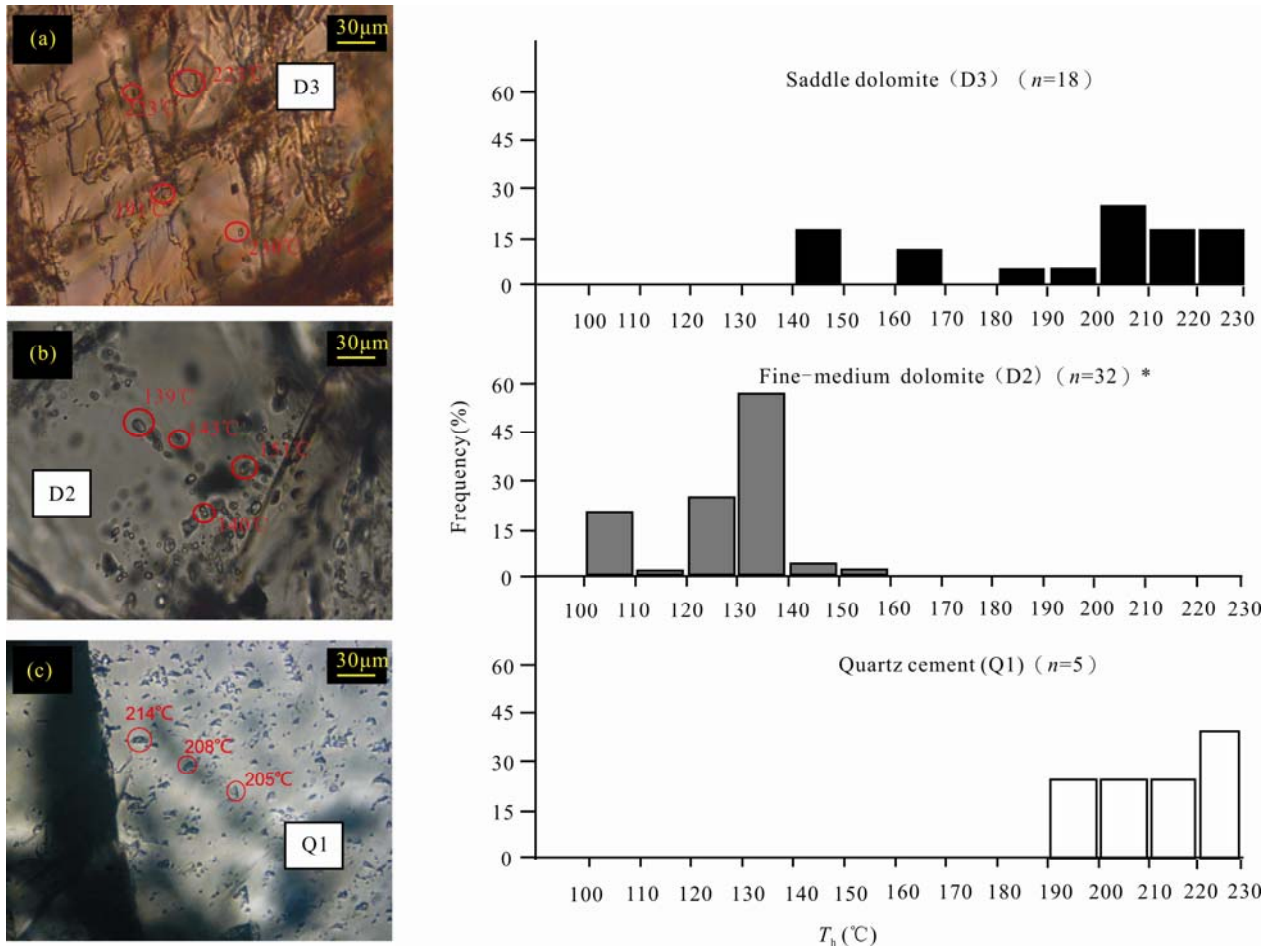


Fig. 5. Micro-characteristics and homogenization temperature (T_h) histogram of fluid inclusions of different fabrics dolomite, Dengying Fm. (data cited from Feng Mingyou et al., 2017).

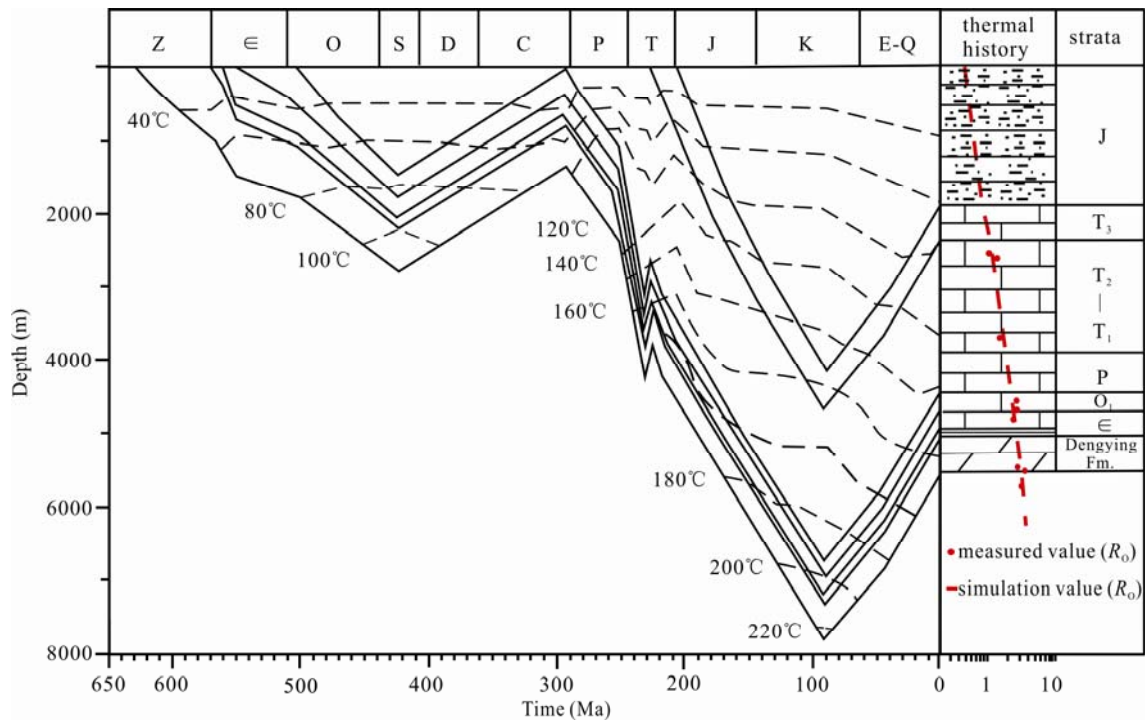


Fig. 6. Burial and thermal history curve graph (based on Well GK1) of the study area (modified from Liu Yifeng et al., 2014).

reformation of hydrothermal fluid, as under high temperature hydrothermal environment, oxygen isotope thermal fractionation occurred (Bai Xiaoliang et al., 2016; Yang Yongqiang et al., 2016), leading to the drastic reduce of $\delta^{18}\text{O}$ but relative increase of $\delta^{16}\text{O}$ in dolomite crystals. Therefore, the saddle dolomite shows lowest $\delta^{18}\text{O}$.

4.2.3 Trace elements and rare earth elements

Generally, the concentration of trace elements in sedimentary fluid and diagenetic fluid is the main factor contributing to the trace elements enrichment in rocks. As previous reports, the diagenetic fluid that affected the micritic dolomite in the Dengying Formation is normal or evaporated seawater. On the contrary, formation of saddle dolomite is attributed to the hydrothermal fluid which comes from deep-burial storage. This difference is directly reflected in the Fe and Mn concentrations of the two different fabrics dolomite mentioned above (Fig. 7a) (Table 1).

The micritic dolomites have the lowest Fe and Mn contents among all the dolomite fabrics, and the

distribution range of Fe is 18 ppm to 152 ppm (average value=71 ppm, $n=8$), and the Mn content range is 80 ppm to 841 ppm (average value=240 ppm, $n=8$). In contrast to the micritic dolomites, the saddle dolomites are enriched in Fe and Mn, and have a average value of 1266 ppm ($n=7$) Fe and 797 ppm ($n=7$) Mn, respectively. The content of Fe and Mn in fine-medium dolomites is between the two dolomite fabrics above. Except for one sample below the detection limit, the distribution range of Fe is 139 ppm to 1946 ppm (average value=482 ppm, $n=11$), and the Mn content range is 134 ppm to 1707 ppm (average value=577 ppm, $n=11$) (Table 1).

Rare earth elements (REE) also record information about diagenetic fluids and diagenetic environment because of its unique geochemical characteristics (Hu Wenxuan et al., 2010). The diagenetic fluids of different origins have distinct REE distribution patterns (Tables 2 and 3). Compared to Neoproterozoic marine limestone (Fig. 8b), all dolomite samples exhibit varying degrees of positive anomalies of Ce (Fig. 8). However, unlike the Neoproterozoic marine limestones, the distribution pattern of fine-medium dolomites and saddle dolomites show

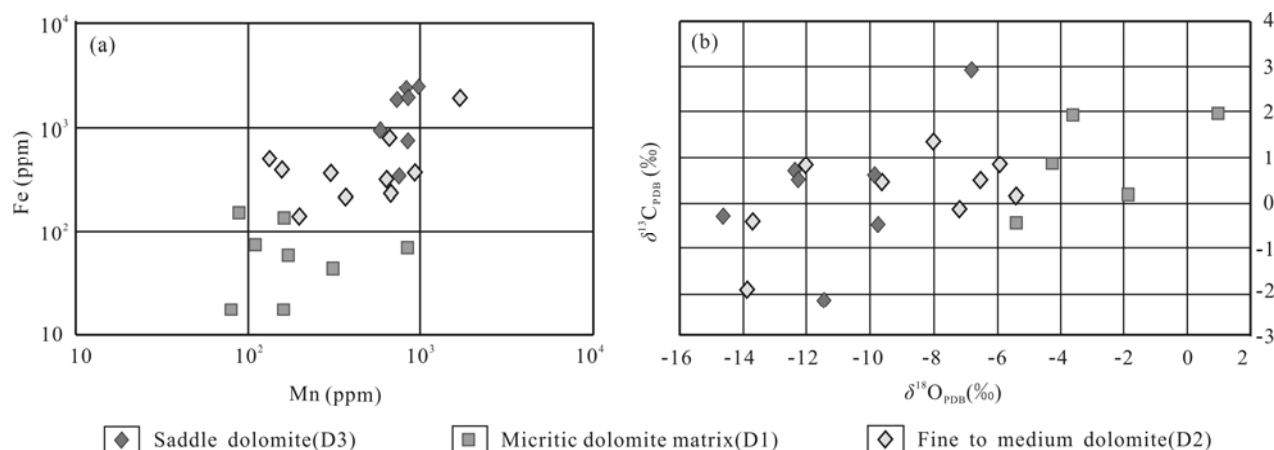


Fig. 7. Fe vs. Mn content (a) and $\delta^{13}\text{C}$ vs. $\delta^{18}\text{O}$ (b) of different fabrics dolomite in hydrothermal dolomite reservoir.

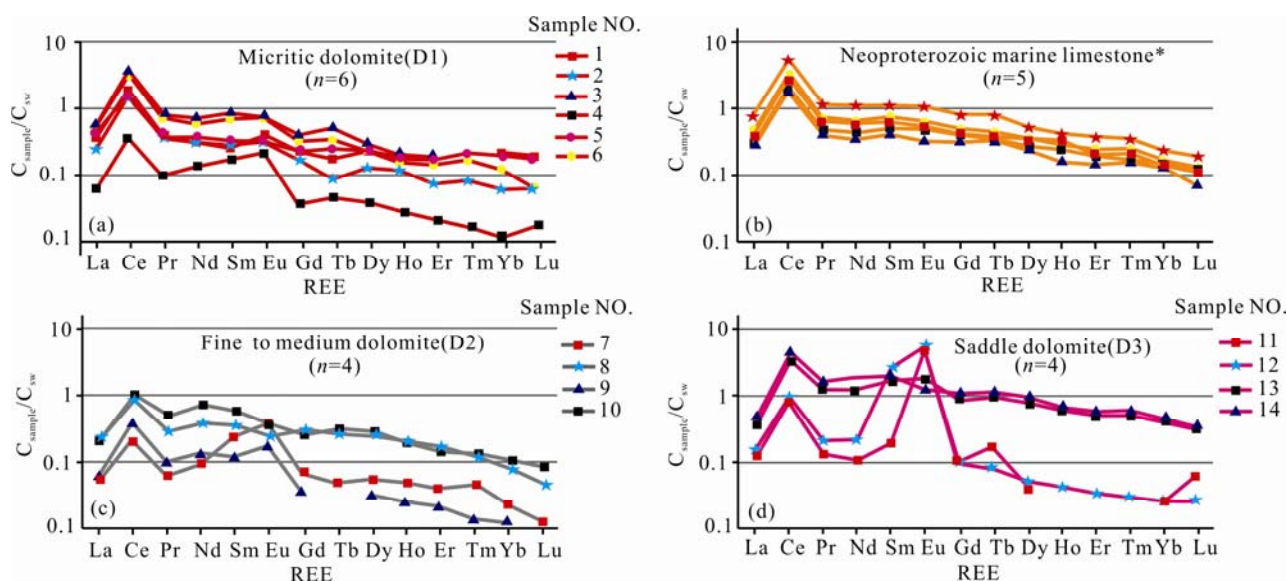


Fig. 8. REE pattern of different fabrics dolomite in member 4th, Dengying Fm. in the study area (Data cited from Sun et al., 2010; Chen Song et al., 2011).

Table 2 Rare earth elements of different fabrics dolomite for member 4th, Dengying Fm. in the study area (1)

Sample No.	Well No.	Depth (m)	Fabric type	La	Ce	Pr	Nd	Sm	Eu	Gd	Tb	Dy	Ho
1	MX9	5433.4	D1	1.33	1.51	0.21	0.75	0.12	0.05	0.16	0.02	0.20	0.05
2	GT2	6264.5	D1	0.83	1.22	0.19	0.76	0.13	0.04	0.12	0.01	0.11	0.03
3	GT2	6266.7	D1	1.79	2.98	0.41	1.67	0.39	0.09	0.29	0.06	0.25	0.05
4	MX39	5303.7	D1	0.21	0.28	0.05	0.31	0.08	0.03	0.03	0.01	0.03	0.01
5	MX9	5433.5	D1	1.52	1.41	0.19	0.87	0.15	0.04	0.17	0.03	0.20	0.04
6	GT2	6267.7	D1	1.83	2.61	0.38	1.41	0.32	0.09	0.24	0.04	0.20	0.04
7	MX39	5266.3	D2	0.18	0.17	0.03	0.22	0.11	0.05	0.05	0.01	0.05	0.01
8	MX39	5272.6	D2	0.77	0.71	0.15	0.96	0.17	0.03	0.22	0.03	0.22	0.05
9	MX39	5302.9	D2	0.21	0.31	0.05	0.32	0.06	0.02	0.03	—	0.03	0.01
10	GS16	5450.2	D2	0.75	0.88	0.26	1.69	0.27	0.05	0.20	0.04	0.26	0.05
11	GT2	6030.8	D3	0.45	0.66	0.07	0.26	0.09	0.61	0.07	0.02	0.04	—
12	GS7	5346.1	D3	1.22	2.70	0.61	2.91	0.79	0.22	0.61	0.11	0.66	0.15
13	GS7	5346.2	D3	1.64	3.55	0.85	4.53	0.90	0.16	0.76	0.14	0.82	0.17
14	GS16	5451.2	D3	0.57	0.81	0.11	0.52	1.22	0.67	0.07	0.01	0.05	0.01

Table 3 Rare earth elements of different dolomite fabrics for Dengying Fm. in the study area (2)

Sample No.	Well No.	Depth (m)	Fabric type	Er	Tm	Yb	Lu	Y	ΣREE+Y	(Nd/Yb) _{SN}	δCe	δEu	δGd
1	MX9	5433.4	D1	0.15	—	0.17	0.03	3.17	7.92	1.55	4.86	1.74	1.10
2	GT2	6264.5	D1	0.06	0.01	0.05	0.01	0.92	4.49	5.33	5.09	1.48	1.10
3	GT2	6266.7	D1	0.16	—	0.13	—	1.75	10.02	4.51	5.77	0.98	0.64
4	MX39	5303.7	D1	0.02	—	0.01	—	0.23	1.28	11.40	4.51	1.75	0.42
5	MX9	5433.5	D1	0.14	0.03	0.16	0.03	3.17	8.15	1.88	4.40	1.04	0.82
6	GT2	6267.7	D1	0.12	0.02	0.10	0.01	1.53	8.94	4.95	5.24	1.25	0.72
7	MX39	5266.3	D2	0.03	0.01	0.02	—	0.96	1.90	4.57	3.72	2.13	0.58
8	MX39	5272.6	D2	0.14	0.02	0.06	0.01	2.70	6.23	5.39	3.51	0.75	1.00
9	MX39	5302.9	D2	0.02	—	0.01	—	0.23	1.30	10.88	4.92	2.17	0.90
10	GS16	5450.2	D2	0.12	0.02	0.08	0.01	2.05	6.73	7.08	3.04	0.74	0.67
11	GT2	6030.8	D3	0.03	—	0.02	0.01	0.40	2.73	4.56	6.33	26.10	0.54
12	GS7	5346.1	D3	0.41	0.06	0.34	0.05	4.75	15.60	4.27	4.43	1.21	0.70
13	GS7	5346.2	D3	0.47	0.07	0.37	0.05	6.85	21.30	3.00	4.23	0.73	0.74
14	GS16	5451.2	D3	0.03	—	0.02	—	0.39	4.48	8.52	5.46	2.98	0.10

significantly positive Eu anomalies which indicate influence of hydrothermal fluids (Ding Zhenju et al., 2000). It can be attributed to the fact that Eu²⁺ and Ca²⁺ have the same valence and similar ion radius that Eu²⁺ would replace the positions of Ca²⁺ in dolomite lattice when water-rock reaction between hydrothermal fluids and micritic dolomite. Consequently, the Eu positive anomaly is formed in the fine-medium dolomite resulting from the recrystallization of micritic dolomite triggered by the water-rock reaction above (Fig. 8).

5 Reservoir Facies Features of Hydrothermal Dolomite Reservoir

Hydrothermal dolomite reservoirs have some macro-characteristics and features similar to the dolomite reservoirs formed by supergene karstification and burial dissolution. However, there are significant differences in two aspects: microscopic petrological characters and inorganic geochemical characteristics. In order to distinguish reservoir types of different origins, a classification table has been established in this study. Based on petrographic and geochemical features, hydrothermal dolomite reservoirs in study area is composed of the following types of reservoir facies.

5.1 Dolomites characterized by hydrothermally dissolved vugs (or pores)

The hydrothermal fluid stored in deep-burial storage consist of clastic rock is characterized by abnormally high temperature and pressure. In the tectonic-hydrothermal

events, these hydrothermal fluids flow upward along faults or concomitant fracture systems formed by strike-slip and transtensional basement-rooted faults. After entering the dilational-breccia zone of “sag” (seismically recognizable depressions at the top surface of hydrothermal dolomite-bearing carbonate formations), the compact micritic dolomite is strongly dissolved with the decrease of temperature and pressure of hydrothermal fluids. After the dissolution process, hydrothermal dissolved pores of which diameter ranges between 200 and 2000 μm and vugs of which diameter larger than 2000 μm (the maximum is 6cm) are formed (Fig. 9). Different from reservoir spaces formed by supergene karstification, hydrothermal dissolved pores and vugs do not distribute in a particular direction, but mainly distribute along the transtensional fractures, and there is no signature cements of underflow zone or vadose zone such as vadose silts, hanging cements, etc. in hydrothermal dissolved pores and vugs but saddle dolomite, quartz and other hydrothermal minerals filling along the rim of pores or vugs. The saddle dolomite crystal is about 300–800 μm in size (the maximum is over 3000 μm), showing fluctuating extinction undercrossed-polarized light and bright light under cathodoluminescence with distinct zonal-structure (Fig. 9).

5.2 Dolomite reservoirs characterized by specific intercrystalline pore

Intercrystalline pores are common in hydrothermal dolomite reservoir. Due to consisting of micritic dolomite crystals (3–5 μm in size), the intercrystalline pores don not exist in Dengying Formation micritic dolomite (host rock).

But when recrystallization of micritic dolomite crystals caused by hydrothermal fluids is completed, complete transformation of the micritic dolomite crystals to euhedral-subhedral dolomite crystals (50–200 μm in size) (Fig. 10c) takes place in the diagenetic process and a large number of intercrystalline pores are formed at the same time (Fig. 11). A large number of bitumen filled in the intercrystalline pores indicates that these pores are effective spaces for hydrocarbon migration and accumulation. Dolomite crystals generated by intense recrystallization may be larger than 200 μm in size and exhibit curved crystal faces, fluctuating extinction under crossed-polarized light (Fig. 10c) and bright light crystal rim under cathodoluminescence (Fig. 10e). These features above cannot be observed on the dolomite crystals of low-

temperature recrystallization.

5.3 Dolomite reservoir characterized by residual inter-breccia vugs (or pore)

The hydraulic fracturing is beneficial to the formation and/or enhancement of the reservoir porosity. The remaining inter-breccia vugs can be retained as a good storage space. The breccia holes are usually completely or incompletely filled with saddle dolomite, and residual breccia holes are retained by incomplete filling (Fig. 12).

5.4 Reservoir characterized by enlarged-fracture due to hydrothermal dissolution

This kind of reservoir space common in study area are structural (or diagenetic) fractures enlarged by dissolution

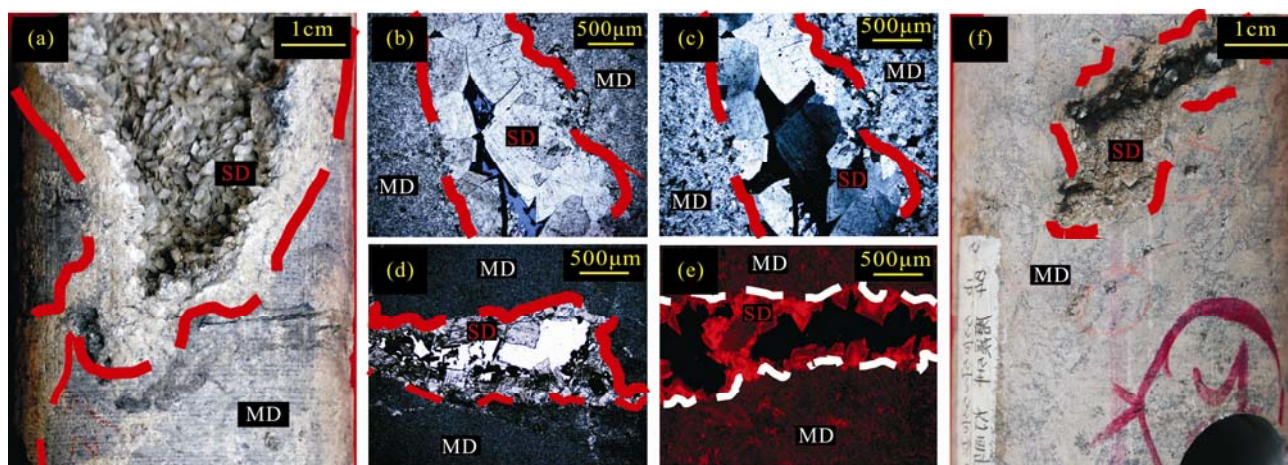


Fig. 9. Petrographic characteristics of hydrothermal dissolved vug (or pore) for member 4th, Dengying Fm..

(a) Vug-filling saddle dolomite (SD) distribute along rim of hydrothermal dissolved vug, Well GS20, 5195.7 m; (b) pore-filling dolomite, with curved or irregular faces, Well GS6, 5035 m, plane-polarized light; (c) well GS6, 5035 m, cross-polarized light; (d) pore-filling saddle dolomite, Well GS1, 4970 m, plane-polarized light; (e) pore-filling saddle dolomite, Well GS1, 4972 m, cathodoluminescence; (f) vug-filling saddle dolomite, Well MX51, 5370.5 m.

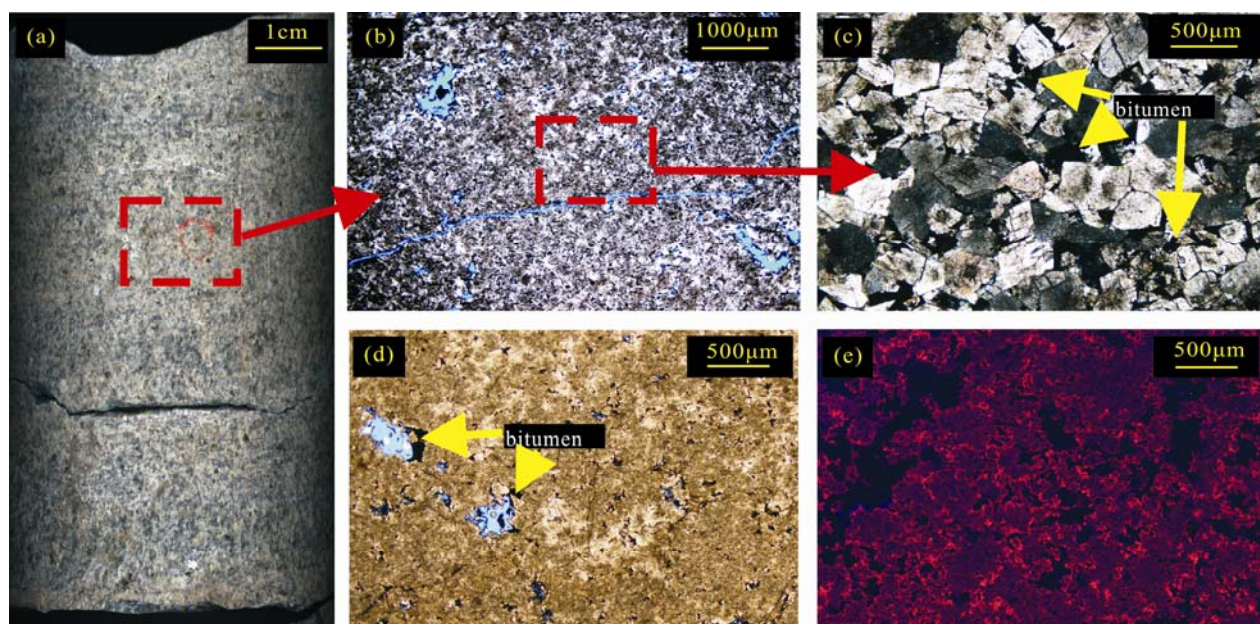


Fig. 10. Petrographic characteristics of intercrystalline pores in member 4th, Dengying Fm..

(a) Core photographs of acicular dissolved pores (intercrystalline pores) in fine-medium dolomite, Well GS16, 5450.62–5450.67 m; (b) Microscopic features of red frame in (a) Well GS16, 5450.65 m, plane-polarized light; (c) Close-up of red frame in (b) showing bitumen filled in intercrystalline pores, Well GS16, 5450.65 m, plane-polarized light; (d) Intercrystalline pores in fine-medium dolomite, Well MX51, 5332.6 m, plane-polarized light; (e) Fine-medium dolomite exhibit dim light and rim of dolomite crystals exhibit bright light, Well MX51, 5332.6m, cathodoluminescence.

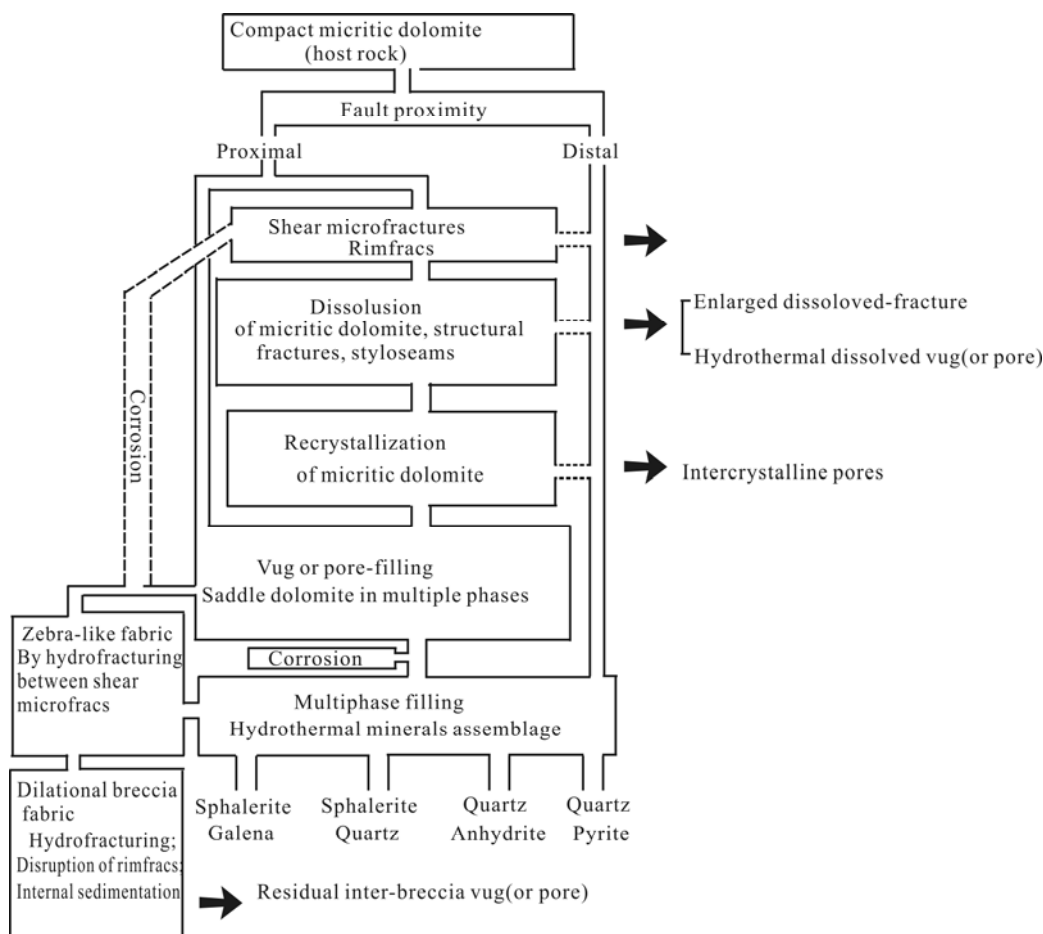


Fig. 11. Diagenetic diagram of hydrothermal diagenesis events in member 4th, Dengying Fm. (modified from Davies et al., 2006).

Table 4 Reservoir types and corresponding signatures of different origins of Dengying Fm.

Reservoir type	Diagenetic fluid	Constructive diagenesis	Reservoir space type	Petrographic features	Typical fillings	Geochemical features of fillings	Cathodoluminescence
Hydrothermal dolomite reservoir	Hydrothermal fluids	Hydrothermal recrystallization	Intercrystalline pores	Occur alone or scatter along fracture rim	Non	High Fe content (925 ppm) high Mn content (650 ppm), high ^{87}Sr , high homogenization temperature (192°C), negative $\delta^{13}\text{C}$ (0.1‰), negative $\delta^{18}\text{O}$ (-11‰) in saddle dolomite	SD-bright light; Qtz, Gn, Sp and Py-non-luminance; Fl-blue light
		Hydrothermal dissolution	Hydrothermal dissolved vug (or pore)	Occur alone or scatter along fracture rim	SD, Qtz, Gn, Sp, Py and Fl		
			Residual inter-breccia vug (or pore)	Occur alone or scatter along fracture rim	SD		
			Enlarged dissolved-fracture	Structural fractures enlarged by corrosion. Irregular rim	SD		
Supergene karst reservoir	Meteoric water	Dissolution and leaching	Karst pore (vug)	Occur in group in a specific direction; fabric selective	VS, HC, and BT	Low Fe content (25 ppm) in botryoidal texture, low Mn content (77 ppm), low ^{87}Sr , abnormally negative $\delta^{13}\text{C}$ and $\delta^{18}\text{O}$ in matrix dolomite*	BT, KB and VS-non-luminance
			Collapse breccia vug		KB, VS and BT		
			melting groove	Structural fractures enlarged by corrosion. Irregular rim	CD, KB, VS and overlying sediments		KB and ambient cements-non-luminance
Burial-dissolution reservoir	Organic acids; H_2S and CO_2 related acids	Burial dissolution	Intercrystalline dissolved pore	Occur along early fractures, pores, vug or stylolites; no fabric selective	CD with poikilitic texture*	Higher $^{87}\text{Sr}/^{86}\text{Sr}$ in grained dolomite than in contemporaneous seawater, negative $\delta^{18}\text{O}$ *	CD fillings -weak light or non-luminance; host rock-non-luminance*
			Intergranular dissolved pore				
			Fracture enlarged by burial and corrosion				

Note: Qtz, Quartz; SD, saddle dolomite; Gn, Galena; Sp, sphalerite; Py, pyrite; Fl, fluorite; VS, vadose silts; HC, hanging cements; BT, botryoidal texture; CD, crystalline dolomite. *The data in the table are average. (data cited from Huang Zhicheng et al., 1999; Zhang Jie et al., 2014).

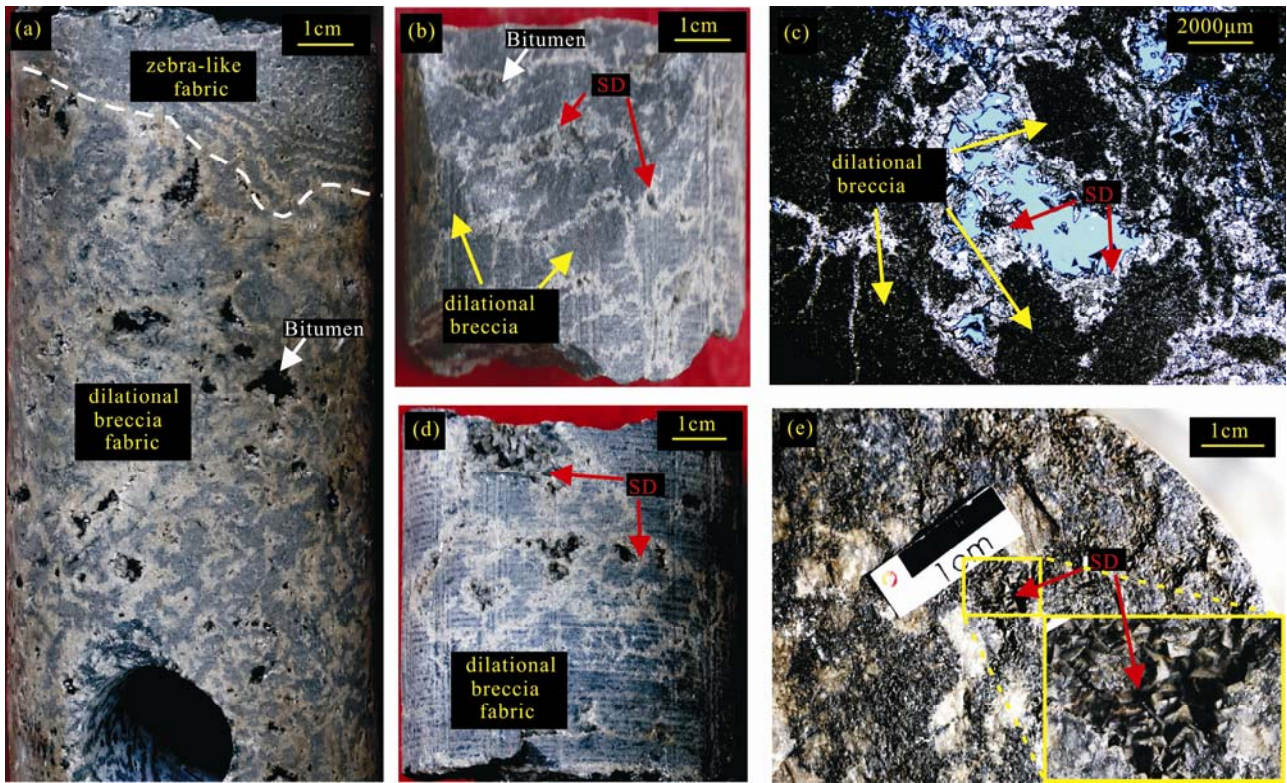


Fig. 12. Petrographic characteristics of residual inter-breccia vugs in Dengying Fm..

(a) The lower part is dilational breccia fabric, the upper part is zebra-like fabric, Well GS111,5324 m; (b) saddle dolomite (SD) and bitumen are sequentially filled in residual inter-breccia vugs, Well GS20,5182.5 m; (c) saddle dolomite (SD) distribute along the rim of residual inter-breccia vugs and pores, Well GS16, 5407.2 m, under plane-polarized light; (d) residual inter-breccia vugs, Well GS20, 5185.4 m; (e) Saddle dolomite (SD) in residual inter-breccia vugsexhibit curved crystal faces, Well MX51, 5335.7 m.

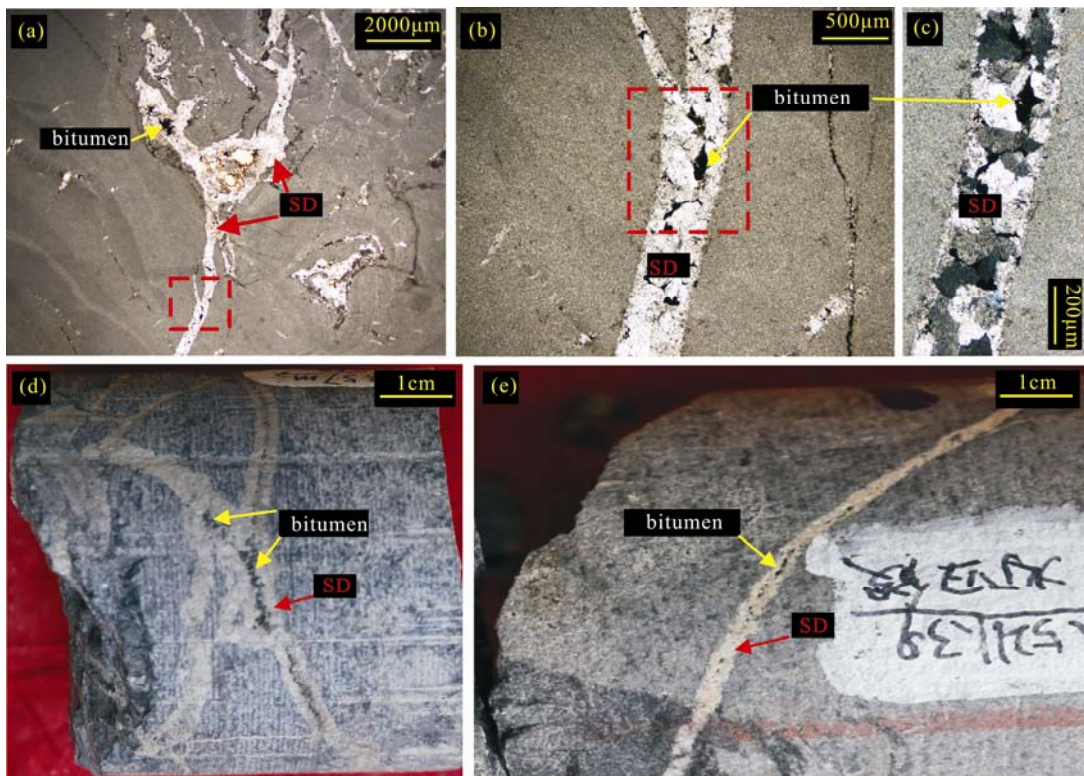


Fig. 13. Petrographic characteristics of enlarged dissolved fractures in Dengying Fm.

(a) Well MX51, 5421.3 m, plane-polarized light; (b) plane-polarized light; (c) well MX23,5211.3 m, cross-polarized light; (d) well GS1, 4972.7 m; (e), well GS1, 4972.7 m.

of hydrothermal fluids (Fig. 13a). They may be partially or entirely filled with saddle dolomite, showing that it is the migration channel of hydrothermal fluids (Fig. 13b). Due to incomplete filling of fractures, the hydrocarbon may still flow through residual space between saddle dolomite crystals and bitumen and precipitated in the end (Fig. 13c).

6 Discussions about the Distribution Model of Hydrothermal Dolomite Reservoir Facies

The development regularity of hydrothermal dolomite reservoirs in limestone formations worldwide demonstrates that a series of geologic effects caused by hydrothermal activities are generally concentrated in: ① circumferential margin of extensional positive faults, especially on fault plates (Lavoie and Morin, 2004); ② basement-rooted strike-slip and transtensional faults, especially at transtensional and dilational structural sites of hanging wall (Davies et al., 2006); ③ The intersection of the above fault (including the conversion fault), especially transtensional “sags” above negative flower structures on wrench faults (Davies et al., 2006; Ding Bozhao et al., 2017; Yang Ping et al., 2017) (Fig. 14). By reprocessing the 3D seismic data with reverse time migration (RTM) and using high-precision coherence analysis, forty-nine transtensional “sags” have been discovered in the study area. These “sags” are hydrothermal channels of multistage hydrothermal reformation (Yang Ping et al., 2017).

In the Lianglitage Formation of Central Tarim Basin, Trenton-Black River Formation of New York (Smith Jr, 2006), Dengying Formation of the study area, and Kometan Formation of the Zagros Basin (Zhang Tao et al., 2015; Feng Mingyou et al., 2017), the correlation between the “Sag” and the development degree of the hydrothermal dolomite reservoir facies is obvious. Therefore, on the basis of satisfying the three basic geological conditions, the development of the hydrothermal dolomite reservoir facies is mainly controlled by the basement-rooted strike-slip and transtensional faults activity.

The two major tectonic hydrothermal fluid activities-Xingkai Taphrogenesis and Emei Taphrogenesis resulted in the vertical development of large basement-rooted faults and lateral development of the grid-like fracture system (Yin Jifeng et al., 2013). The findings of the latest seismic research illustrate that a large range of strike-slip faults and hydrothermal channels exist in the study area and seismic sections are characterized by transtensional “sags” (Yang Zhiru et al., 2014; Ding Bozhao et al., 2016; Yang Ping et al., 2017). High-temperature fluids flow upward along those migration channels consist of faults and concomitant fractures to dissolve, hydraulic fracturing or recrystallize the compact micritic dolomite (host rock). In addition, with the overlying Qiongzhusi Formation black shale which is a few hundred meters in thickness serving as a competent sealing mechanism, the residence of the hydrothermal fluids in the Dengying Formation can be prolonged to facilitate extended diagenetic reactions which form hydrothermal dolomite reservoir facies.

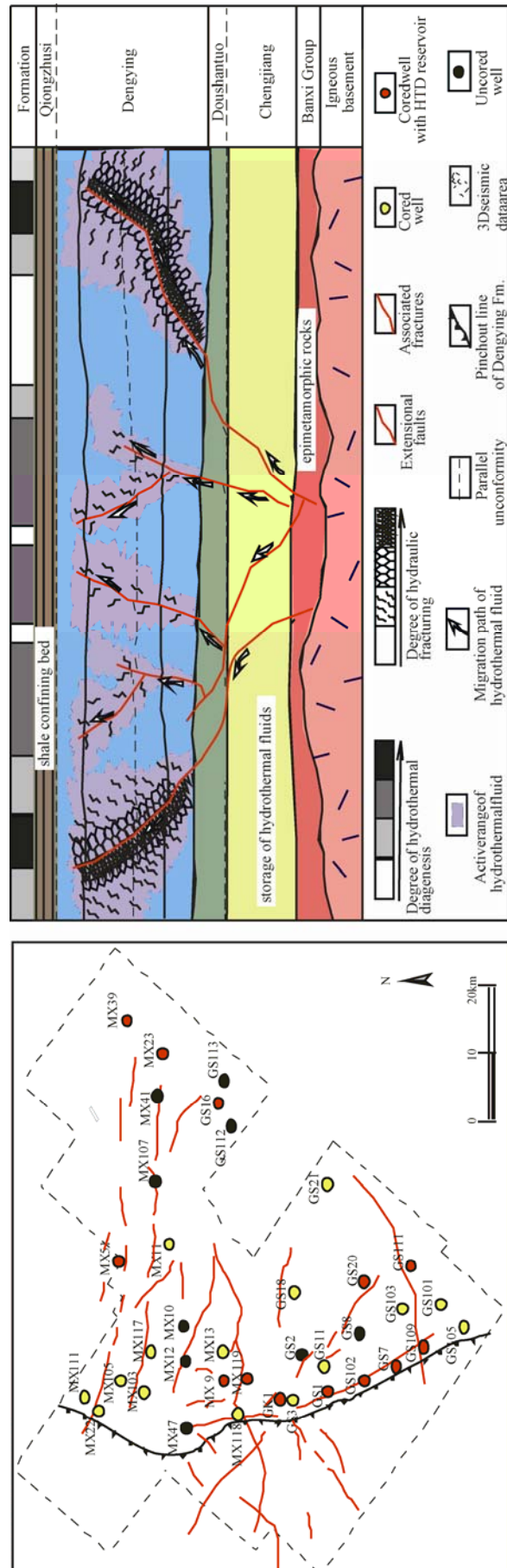


Fig. 14. Conceptual distribution model of hydrothermal dolomite reservoirs for Dengying Formation in the study area.

7 Conclusions

(1) Hydrothermal mineral assemblages such as saddle dolomite-quartz-anhydrite, saddle dolomite-galenasphealerite, saddle dolomite-pyrite-quartz, etc. are common in the Precambrian Dengying Formation in Central Sichuan Basin, SW China. Combined with geochemical characteristics (including homogenization temperature, trace elements and rare earth elements, and isotopes), it is indicated that hydrothermal dolomite reservoirs exist in Dengying Formation, which consist of four types of reservoir spaces including hydrothermal dissolved vug (or pore), intercrystalline pore, residual inter-breccia vug (or pore) and enlarged dissolved-fracture.

(2) Based on the petrographic and geochemical characteristics of three dolomite fabrics in hydrothermal dolomite reservoirs, namely, saddle dolomite, fine-to-medium dolomite and micritic dolomite, it is concluded that saddle dolomite with curved or irregular crystal faces were directly crystallized from high-temperature hydrothermal fluids (average value 192°C); fine-medium dolomite are products of hydrothermal recrystallization for micritic dolomite, resulting in abnormal geochemical indicator of dolomite with slightly depletion of $\delta^{18}\text{O}$ and enrichment of Mn, Fe and $^{87}\text{Sr}/^{86}\text{Sr}$; zebra-like fabric and dilational breccia fabric are the results of hydraulic fracturing during hydrothermal activity. The constructive diagenesis of hydrothermal activity for micritic dolomite in Dengying Formation include hydrothermal dissolution, recrystallization and hydraulic fracturing.

(3) A distribution model of hydrothermal dolomite reservoirs has been proposed, including three basic geological conditions: (a) extensional movements and tectonic-hydrothermal events-The Xingkai Taphrogenesis of Late Sinian-Early Cambrian and Emei Taphrogenesis of Late Permian; (b) the hydrothermal fluid storage consist of clastic rocks with large thickness-Nanhua System Chengjiang Formation and part of Doushantuo Formation; (c) confining bed for hydrothermal fluids-Qiongzhusi Formation shale. Large basement-rooted faults include extensional faults and strike-slip faults, which offer pathways for upward migration of hydrothermal fluids. Associated grid-like fracture system may function as the channels for hydrothermal fluid flow. The intersection of the above faults (including the conversion fault), especially transtensional sags above negative flower structures on wrench faults can serve as a key target for future hydrocarbon exploration.

Acknowledgements

This study was funded by the National Science and Technology Major Project (grant No. 2016ZX05052) and the National Natural Science Foundation of China (grant No. 41072102).

Manuscript received June 20, 2018
accepted Aug. 20, 2018
associate EIC XIAO Yitian
edited by HAO Qingqing

References

- Bai Xiaoliang, Zhang Shaonan, Huang Qingyu, Ding Xiaoqi and Zhang Siyang, 2016. Origin of dolomite in the Middle Ordovician peritidal platform carbonates in the northern Ordos Basin, western China. *Petroleum Science*, 13(3): 434–449.
- Cervato, C., 1990. Hydrothermal dolomitization of Jurassic-Cretaceous limestones in the southern Alps (Italy): relation to tectonics and volcanism. *Geology*, 18(5): 458–461.
- Cocherie, A., Calvez, J.Y., and Oudin-Dunlop, E., 1994. Hydrothermal activity as recorded by Red Sea sediments: Sr-Nd isotopes and REE signatures. *Marine Geology*, 118(3–4): 291–302.
- Chen Daizhao, 2008. Structure-controlled hydrothermal dolomitization and hydrothermal dolomite reservoirs. *Oil & Gas Geology*, 29(5): 614–622 (in Chinese with English abstract).
- Conliffe, J., Azmy, K., Knight, I., and Lavoie, D., 2009. Dolomitization of the Lower Ordovician Watts Bight Formation of the St. *Canadian Journal of Earth Sciences*, 46(4): 247–261.
- Chen Song, Gui Herong, Sun Linhua, Liu Xianghong and Ma Yanping, 2011. Geochemical characteristics of REE in limestone of Jiudingshan Formation, northern Anhui Province and their constraint on the seawater. *Geology in China*, 38(3): 664–672 (in Chinese with English abstract).
- Ding Zhenju, Liu Congqiang, Yao Shuzhen and Zhou Zonggui, 2000. Rare earth elements compositions of high-temperature hydrothermal fluids in sea floor and control factors. *Advance in Earth Sciences*, 15(3): 307–312 (in Chinese with English abstract).
- Davies, G.R., and Smith Jr, L.B., 2006. Structurally controlled hydrothermal dolomite reservoir facies: an overview. *AAPG Bulletin*, 90(11): 1641–1690.
- Ding Bozhao, Zhang Guangrong, Chen Kang, Geng Wei, Zhu Xinghui and Fan Chang, 2017. Genesis research of collapsed-paleo-cave systems in Sinian carbonate strata in Central Sichuan Basin, SW China. *Natural Gas Geoscience*, 28(8): 1–8 (in Chinese with English abstract).
- Fairchild, J.J., and Spiro, B., 1987. Petrological and isotopic implications of some contrasting late Precambrian carbonate, NE Spitsbergen. *Sedimentology*, 34(6): 793–989.
- Feng Mingyou, Qiang Zitong, Shen Ping, Zhang Jian, Tao Yanzhong and Xia Maolong, 2016. Evidences for hydrothermal dolomite of Sinian Dengying Formation in Gaoshiti-Moxiarea, Sichuan Basic. *Acta Petrolei Sinica*, 37(5): 587–598 (in Chinese with English abstract).
- Feng Mingyou, Wu Pengcheng, Qiang Zitong, Liu Xiaohong, DuanYong and Xia Maolong, 2017. Hydrothermal dolomite reservoir in the Precambrian Dengying Formation of Central Sichuan Basin, Southwestern China. *Marine and Petroleum Geology*, 82: 206–219.
- Goldstein, R.H., and Reynolds, T.J., 1994. Systematics of fluid inclusions in diagenetic minerals: *SEPM Short Course*, 31: 1–199.
- Hurley, N. F., and Budros, R., 1990. Albion-Scipio and Stoney Pointfields—U.S.A. Michigan Basin, in E. A. Beaumont and N. H. Foster, eds., *Stratigraphic traps I: AAPG Treatise of Petroleum Geology, Atlas of Oil and Gas Fields*: 1–37.
- Huang Zhicheng, Chen Zhina, Yang Shouye and Liu Yan, 1999. Primary $\delta^{13}\text{C}$ and $\delta^{18}\text{O}$ values in marine carbonates and the sea water temperature of Dengyingxia age in South China. *Journal of Palaeogeography*, 1(3): 1–7 (in Chinese with English abstract).
- Hu Wenxuan, Chen Qi, Wang Xiaolin and Cao Jian, 2010. REE models for the discrimination of fluids in the formation and evolution of dolomite reservoirs. *Oil & Gas Geology*, 31(6): 810–818 (in Chinese with English abstract).
- Huang Sijing, 2010. Carbonate diagenesis. *Beijing: Geological Publishing House*, 268 (in Chinese).
- Inoue, A., 1995. Formation of clay minerals in hydrothermal environments in Velde B. (eds). Origin and mineralogy of clays-clays in the environment. *Springer, Berlin, Heidelberg*, 268–329.
- Jin Zhijun, Zhu Dongya, Hu Wenxuan, Zhang Xuefeng, Wang Yi

- and Yan Xiangbin, 2006. Geological and geochemical signatures of hydrothermal activity and their influence on carbonate reservoir beds in the Tarim Basin. *Acta Geologica Sinica*, 80(2): 245–253 (in Chinese with English abstract).
- Jiang Yuqiang, Tao Yanzhong, Gu Yifan, Wang Juebo, Qiang Zitong, Jiang Na, Lin Gang and Jiang Chan, 2016. Hydrothermal dolomitization in Dengying Formation, Gaoshiti-moxi area, Sichuan Basin, SW China. *Petroleum Exploration and Development*, 43(1): 54–64.
- Kawabe, I., Toriumi, T., Ohta, A., and Miura, N., 1998. Monoisotopic REE abundances in seawater and the origin of seawater tetrad effect. *Geochemical Journal*, 32(4): 213–229.
- Lavoie, D., and Morin, C., 2004. Hydrothermal dolomitization in the Lower Silurian Sayabec Formation in northern Gaspé-Matapédia (Québec): constraint on timing of porosity and regional significance for hydrocarbon reservoirs. *Bulletin of Canadian Petroleum Geology*, 52(3): 256–269.
- Lonnee, J., and Machel, H., 2006. Pervasive dolomitization with subsequent hydrothermal alteration in the Clarke Lake gas field, Middle Devonian Slave Point Formation, British Columbia, Canada. *AAPG Bulletin*, 90(11): 1739–1761.
- Luczaj, J.A., Harrison III, W.B., and Williams, N.S., 2006. Fractured hydrothermal dolomite reservoirs in the Devonian Dundee Formation of the Central Michigan Basin. *AAPG Bulletin*, 90(11): 1787–1801.
- Liu Shugen, Ma Yongsheng, Huang Wenming, Cai Xunyu, Zhang Changjun, Wang Guo zhi, Xu Guosheng, Yong Ziquan and Pan Changlin, 2007. Densification process of Upper Sinian Dengying Formation, Sichuan Basin. *Natural Gas Geoscience*, 18(4): 485–496 (in Chinese with English abstract).
- Liu Shugen, Huang Wenming, Chen Cuihua, Zhang Changjun, Li Juchu, Dai Sulan and Qin Chuan, 2008. Primary study on hydrothermal fluids activities and their effectiveness on petroleum and mineral accumulation of Sinian system—Palaeozoic in Sichuan Basin. *Journal of Mineralogy & Petrology*, 28(3): 41–50.
- Luo Zhili, 2009. Emei Taphrogenesis and natural gas prospecting practices in Sichuan Basin. *Xinjiang Petroleum Geology*, 30: 419–424 (in Chinese with English abstract).
- Lavoie, D., and Chi, G., 2010. Lower Paleozoic foreland basins in eastern Canada: tectono-thermal events recorded by faults, fluid and hydrothermal dolomites. *Bulletin of Canadian Petroleum Geology*, 58(1): 17–35.
- Lapponi, F., Bechstädt, T., Boni, M., Banks, D.A., and Schneider, J., 2013. Hydrothermal dolomitization in a complex geodynamic setting (Lower Palaeozoic, Northern Spain). *Sedimentology*, 61(2): 411–443.
- Li Qigui, Li Kesheng, Zhou Zhuozhu, Yan Jihong and Tang Huanyang, 2013. Palaeogeomorphology and karst distribution of Tongwan unconformity in Sichuan Basin. *Oil and Gas Geology*, 34(4): 516–521 (in Chinese with English abstract).
- Liu Yifeng, Qiu Nansheng, Xie Zengye, Yao Qianying and Wu Bin, 2014. Characteristics and effects on gas accumulation of the Sinian-Lower Cambrian temperature-pressure field in the central paleo-uplift, Sichuan Basin. *Acta Sedimentologica Sinica*, 32(3): 601–610 (in Chinese with English abstract).
- Luo Bing, Yang Yueming, Luo Wenjun, Wen Long, Wang Wenzhi and Chen Kang, 2015. Controlling factors and distribution of reservoir development in Dengying Formation of paleo-uplift in Central Sichuan Basic. *Acta Petrolei Sinica*, 36(4): 416–426 (in Chinese with English abstract).
- Liu Wei, Huang Qingyu, Wang Kun, Shi Shuyuan and Jiang Hua, 2016. Characteristics of hydrothermal activity in the Tarim Basin and its reworking effect on Carbonate reservoirs. *Natural Gas Industry*, 36(3): 14–21 (in Chinese with English abstract).
- Lin Xiaoxian, Peng Jun, Du Lingchun, Yan Jianping and Hou Zhongjian, 2017. Characterization of the microbial dolomite of the Upper Sinian Dengying Formation in the Hanyuan area of Sichuan Province, China. *Acta Geologica Sinica* (English Edition), 91(3): 806–821.
- Matsumoto, R., Iijima, A., and Katayama, T., 1988. Mixed-water and hydrothermal dolomitization of the Pliocene Shirahama Limestone, Izu Peninsula, central Japan. *Sedimentology*, 35 (6): 979–998.
- Malone, M.J., Baker, P.A., and Burns, S.J., 1996. Hydrothermal dolomitization and recrystallization of dolomite breccias from the Miocene Monterey Formation, Tepusquet area, California. *Journal of Sedimentary Research*, 66(5): 976–990.
- Nurkhanuly, U., and Dix, G.R., 2014. Hydrothermal dolomitization of Upper Ordovician limestone, Central-East Canada: fluid flow in a craton-interior wrench-fault system likely driven by distal tectonic tectonism. *Journal of Geology*, 122: 259–282.
- Ostendorf, J., Henjes-Kunst, F., Mondillo, N., Boni, M., Schneider, J., and Gutzmer, J., 2016. Formation of Mississippi valley-type deposits linked to hydrocarbon generation in extensional tectonic settings: evidence from the Jabali Zn-Pb-(Ag) deposit (Yemen). *Geology*, 43(12): 1055–1058.
- Phillips, W.J., 1972. Hydraulic fracturing and mineralization. *Journal of the Geological Society*, 128: 337–359.
- Pan Wenqing, Liu Yongfu, Dickson, J.A.D., Shen Anjiang, Han Jie, Ye Ying, Gao Hongliang, Guan Ping, Zhang Lijuan and Zheng Xingping, 2009. The geological model of hydrothermal activity in outcrop and the characteristics of carbonate hydrothermal karst of Lower Paleozoic in Tarim Basin. *Acta Sedimentologica Sinica*, 27: 983–994 (in Chinese with English abstract).
- Qing, H.R., and Mountjoy, E.W., 1992. Large-scale fluid flow in the Middle Devonian Presquile barrier, Western Canada Sedimentary Basin. *Geology*, 20: 903–906.
- Qing, H.R., and Mountjoy, E.W., 1994. Formation of coarsely crystalline, hydrothermal dolomite reservoirs in the Presquile Barrier, Western Canada Sedimentary Basin. *AAPG Bulletin*, 78(1): 55–77.
- Yin Jifeng, Gu Zhidong and Li Qiufen, 2013. Characteristics of deep-rooted faults and their geological significances in Dachuanzhong area, Sichuan Basin. *Oil and Gas Geology*, 34 (3): 376–382 (in Chinese with English abstract).
- Roehl, P.O., 1981. Dilation brecciation: a proposed mechanism of fracturing, petroleum expulsion and dolomitization in the Monterey Formation, California. *AAPG Bulletin*, 65: 980–981.
- Ronchi, P., Masetti, D., Tassan, S., and Camocino, D., 2012. Hydrothermal dolomitization in platform and basin carbonate successions during thrusting: a hydrocarbon reservoir analogue (Mesozoic of Venetian Southern Alps, Italy). *Marine and Petroleum Geology*, 29(1): 68–89.
- Stoffregen, R., 1987. Genesis of acid-sulfate alteration and Au-Cu-Ag mineralization at Summitville, Colorado. *Economic Geology*, 82: 1575–1591.
- Smith, Jr, L.B., 2006. Origin and reservoir characteristics of Upper Ordovician Trenton–Black river hydrothermal dolomite reservoirs in New York. *AAPG Bulletin*, 90(11): 1691–1718.
- Sun Linhua, Gui Herong and He Zhenyu, 2010. Rare earth element characteristics of the Neoproterozoic limestones in Lingbi District, Northern Anhui Province. *Chinese Rare Earths*, 31(6): 32–40 (in Chinese with English abstract).
- Song Guangyong, Liu Shugen, Li Senming and Wang Pengcheng, 2011. Origin of Dengying saddle dolomite in well Lin -1 in southeastern part of Sichuan Basin. *Marine Origin Petroleum Geology*, 16(2): 53–60 (in Chinese with English abstract).
- Shah, M.M., Nader, F.H., Garcia, D., Swennen, R., and Ellam, R., 2012. Hydrothermal dolomites in the Early Albian (Cretaceous) platform Carbonates (NW Spain): nature and origin of dolomites and dolomitizing fluids. *Oil & Gas Science & Technology*, 67: 97–122.
- Tarasiewicz, J.P.T., Woodcock, N.H., and Dickson, J.A.D., 2005. Carbonate dilation breccias: examples from the damage zone to the dent fault, Northwest England. *Geological Society of America Bulletin*, 117(5): 736–745.
- Wang Guozhi, Liu Shugen, Li Na, Wang Dong and Gao Yuan, 2014. Formation and preservation mechanism of high quality reservoir in deep burial dolomite in the Dengying Formation on the northern margin of the Sichuan Basin. *Acta Petrologica Sinica*, 30(3): 667–678.
- Xu Fanghao, Xu Guosheng, Liang Jiaju, Yuan Haifeng, Liu Yong and Xu Fanggen, 2016. Multi-stage fluid charging and critical

- period of hydrocarbon accumulation of the Sinian Dengying Formation in central Sichuan Basin. *Acta Geologica Sinica* (English Edition), 90(4): 1549–1550.
- Yang, J., Sun, W., Wang, Z., Xue, Y., and Tao, X., 1999. Variations in Sr and C isotopes and Ce anomalies in successions from China: evidence for the oxygenation of Neoproterozoic seawater? *Precambrian Research*, 93: 215–233.
- Yang Wei, Wei Guoqi, Zhao Rongrong, Liu Mancang, Jin Hui, Zhao Zuoan and Shen Juehong, 2014. Characteristics and distribution of karst reservoirs in the Sinian Denying Fm, Sichuan Basin. *Natural Gas Industry*, 34(3): 55–60 (in Chinese with English abstract).
- Yang Zhiru, Wang Xuejun, Feng Xukui, Ji Xuewu, Xu Hu and Li Mingyi, 2014. Geological research and significance of a rift valley in the Presinian period in Central Sichuan Basin. *Natural Gas Industry*, 34(3): 80–85 (in Chinese with English abstract).
- Yang Ping, Ding Bozhao, Fan Chang, Zhu Xinghui, Wang Yajing and Yang Pei, 2017. Distribution pattern and origin of the columnar pull-down anomalies in Gaoshiti Block of Central Sichuan Basin, SW China. *Petroleum Exploration and Development*, 44(3): 370–379.
- Yang Yongqiang, Qiu Longwei, Jay Gregg, Shi Zheng and Yu Kuanhong, 2016. Formation of fine crystalline dolomites in lacustrine carbonates of the Eocene Sikou depression, Bohai Bay Basin, East China. *Petroleum Science*, 13(4): 642–656.
- Zhu Dongya, Jin Zhijun and Hu Wenxuan, 2010. Hydrothermal recrystallization of the Lower Ordovician dolomite and its significance to reservoir in Northern Tarim Basin. *Science China Earth Science*, 40(2): 156–170.
- Zhang Jian., Shen Ping, Yang Wei, Yang Yu and Zeng Fuying, 2012. New understandings of Pre-Sinian sedimentary rocks in the Sichuan Basin and the significance of oil and gas exploration there. *Natural Gas Industry*, 32(7): 1–5 (in Chinese with English abstract).
- Zhang Jie, Brian Jones, Pan Liyin, Zhou Jingao, Qin Yujuan, Hao Yi and Wu Mingde, 2014. Origin of botryoidal dolostone of the Sinian Dengying Formation in Sichuan Basin. *Journal of Palaeogeography*, 16(5): 715–725.
- Zhang Tao, Su Yushan, She Gang, Ahemaitijiang and Zhang Demin, 2015. A study on the genetic model of hydrothermal dolomitization in TaqTaq oilfield, Kurdistan region, Iraq-Taking oilfield A in the Cretaceous in Zagros Basin as an example. *Oil and Gas Geology*, 36(3): 393–401 (in Chinese with English abstract).
- Zi Jinping, Jia Dong, Wei Guoqi, Yang Zhenyu, Zhang Yong, Hu Jing and Shen Shuxin, 2017. LA-ICP-MS U-Pb zircon ages of volcanic clastic beds of the third member of the Sinian (Ediacaran) Dengying Formation in Leshan, Sichuan, and a discussion on the rift evolution in the basin. *Geological Review*, 63: 1040–1049 (in Chinese with English abstract).

About the first author

GU Yifan, male, born in 1990 in Hebei Province of China, is a Ph. D. candidate of Southwest Petroleum University. He is mainly engaged in researches of carbonate sedimentology, dolomitization mechanism and hydrocarbon charge. E-mail: 514468587@qq.com.



About the corresponding author

JIANG Yuqiang, male, born in 1963, received his M.S. degree in 1993 from the Southwest Petroleum University, and is now a professor of geology at the Southwest Petroleum University. His current interests include the study of dolomitization mechanism and hydrocarbon accumulation in sedimentary basins. He has published about 40 papers on the depositional pattern and diagenesis of carbonates of the Sichuan and Tarim Basins. E-mail: xnsyjyq3055@126.com.

